Electronic structure of wide-band-gap ternary pnictides with the chalcopyrite structure

A. G. Petukhov, W. R. L. Lambrecht, and B. Segall
Department of Physics, Case Western Reserve University, Cleveland, Ohio 44106-7079
(Received 26 October 1993)

Electronic band structures, equilibrium lattice constants and structural parameters, cohesive energies, and bulk moduli calculated by means of the linear-muffin-tin-orbital method are presented for $BeCN_2$, $MgCN_2$, $BeSiN_2$, $MgSiN_2$, and $MgSiP_2$ in the chalcopyrite structure. The relationships of these compounds to the "parent" III-V compounds are clarified.

I. INTRODUCTION

This paper presents a theoretical study that we initiated on a class of wide-band-gap semiconductors with chemical formula II-IV-V_2, including carbonitrides, siliconitrides, and one silicophosphide, having the chalcopyrite structure. Using first principles calculations for the total energy, the lattice is allowed to fully relax. This allows for the determination of all structural parameters, the cohesive energies, and bulk moduli, as well as the electronic band structures.

The motivation for this study comes from several recent developments. First of all, there has been an increasing interest in wide-band-gap semiconductors,[1] among which are the group-III nitrides (*c*-BN, AlN, GaN, InN). A member of the class of materials that we study here can be pictured as being derived from a III-N compound by replacing every other group-III element by a group-II element (e.g., Be, Mg, Zn) and the other one by a group-IV element (e.g., C, Si). The octet rule of chemical bonding clearly remains satisfied by this substitution and one may thus expect these materials to have similar tetrahedrally coordinated structures. By analogy to the corresponding II-SiP_2 and II-GeP_2 compounds, the chalcopyrite structure appears to be a plausible candidate crystal structure.

Among the ternary compounds having the chalcopyrite structure, $ZnGeP_2$ is currently being studied intensively for its promising nonlinear optics applications.[2] The favorable properties of this group of semiconductors for second-harmonic generation were predicted by Levine.[3]

Also, it was recently proposed that II-IV-V_2 compounds could be useful as buffer layers in heterovalent epitaxial growth. Alerhand *et al.*[4] suggested that the interface charge neutrality would be more easily satisfied by these materials grown on Si{001} than by GaAs. Their argument is simply based on the electron count per bond. A similar effect may thus be expected for II-SiN_2 materials in the growth of AlN and GaN on Si (or on SiC). The resulting structure of say $MgSiN_2$ on Si {001} would actually not be the chalcopyrite structure, but rather a fairly similar {001} 1 + 1 superlattice of $(MgN)_1(SiN)_1$. Although this would only seem to defer the charge neutrality problem to the $MgSiN_2$/GaN interface, the important point may be facilitating the initial stages of planar growth. One might then envision a gradual change from the $MgSiN_2$ to AlN or GaN. The carbonitrides and siliconitrides thus might be of interest as buffer layers for improving III-N growth.

In addition, the proposed compounds may have more interesting and perhaps even superior optical properties than the III nitrides themselves. For example, they may have larger nonlinear coefficients and they may have direct band gaps in cases where the parent compound has an indirect band gap (e.g., *c*-BN and ZB-AlN; see below). To our knowledge $BeCN_2$ and $MgCN_2$ compounds have not yet been synthesized, while $BeSiN_2$ and $MgSiN_2$ were synthesized in a structure derived from the wurtzite structure[5,6] which is very similar to the chalcopyrite structure. More precisely this structure is built from the same elementary atomic tetrahedra, but since the arrangement of these tetrahedra is wurtzitelike, it has 32 atoms per unit cell. It is thus reasonable to expect that the cohesive and elastic properties as well as general trends in the electronic structure of $BeSiN_2$ and $MgSiN_2$ can be described very well by those they would have in the chalcopyrite structure. Moreover, it is quite possible that these materials can be grown in the chalcopyrite phase. That is why some guidance from theory as to what lattice constants, elastic properties, and band structures one can expect for these materials should be very useful. Knowledge about these properties is important for selecting epitaxial pairs with minimal lattice-constant mismatch and for the identification and characterization of these new compounds.

We previously published the results of a study of $BeCN_2$ in the chalcopyrite structure.[8] Further work on this material and on the $MgCN_2$ in the {001} layered superlattice is in progress.

Previous first principle calculations of a number of II-IV-V_2 compounds other than the nitrides (but including $MgSiP_2$ which is considered here) were performed by Continenza *et al.*[9] Using experimental values of the lattice constants a and c, these authors determined the internal distortion parameter u (defined below). Prior to that Zunger and Jaffe reported first principles results for a series of chalcopyrites compounds, i.e., the ternary compounds I-III-VI_2,[10] with I=Cu,Ag and for $InGaP_2$.[11]

II. COMPUTATIONAL METHOD

The computational method employed in this work is the density functional theory[12] in the local density approximation (LDA) with Hedin-Lundqvist exchange and correlation.[13] The linear muffin-tin-orbital (LMTO) method[14] is used in the atomic sphere approximation (ASA) including both the combined correction term and the muffin-tin (MT) or Ewald correction.[15] As usual for tetrahedrally bonded solids, empty spheres are introduced in the tetrahedral interstices.[16]

The calculations were performed nonrelativistically since only light elements are involved. The Brillouin zone integrations were performed with a special k-point set of 11 Monkhorst-Pack[17] points or with a regular tetrahedron mesh of 59 points in the irreducible part of the zone. These were found to give equally well-converged results. The MT correction was found to be necessary to obtain meaningful behavior of the total energy as a function of the internal structural degree of freedom u (described below) and the c/a ratio. This correction must be distinguished from the combined correction term. The latter corrects the overlap matrix for the geometric error associated with the slightly overlapping spheres and for the neglect of higher partial waves in the expansions of the muffin-tin tails inside the spheres. The ASA total energy includes an electrostatic term arising from the interactions between the point charges associated with the net charge per sphere. In the MT approach, the doubly counted charge in the overlap region of the spheres is corrected for by calculating the electrostatic energy corresponding to that of charged spheres in a uniform background charge density. The latter is estimated from the charge density at the sphere radius. This approach has been found to give important improvements for relaxation calculations of c/a in a tetragonal form of CsI,[18] metal structural energy differences,[18,19] and the transverse optical phonon in Si.[20] We test the approach on a compound having the chalcopyrite structure for which the structure parameters are known, $MgSiP_2$.[21]

III. CRYSTAL STRUCTURE

The chalcopyrite structure ABC_2 is a body centered tetragonal (bct) lattice which has eight atoms per unit cell. It can be thought of as a tetragonally distorted A_2B_2 (or $2+2$) face centered cubic (fcc) superlattice in the {201} direction of the cations A and B with an interpenetrating fcc lattice of common anions C displaced by $(1/4, 1/4, u)$. The structural parameters are the lattice constant a [corresponding to the cubic lattice constant of the zinc-blende (ZB) structure from which the chalcopyrite is derived], the $\eta = c/a$ ratio, and the internal displacement parameter u. In the ideal structure $\eta = 2$ and $u = 1/4$. In terms of these parameters, the bond lengths are given by

$$d_{AC} = a\sqrt{u^2 + (1/4)^2 + (\eta/8)^2},$$
$$d_{BC} = a\sqrt{[u - (1/2)]^2 + (1/4)^2 + (\eta/8)^2}. \quad (1)$$

The total energy in the present calculations was minimized as a function of the three structural parameters. The approach followed was to minimize the energy for fixed a by successive steps on a mesh of u and η values and then to vary a. With u and η fixed at their equilibrium value, the Rose *et al.*[22] equation of state was then fitted to the $E(a)$ curves in order to determine the equilibrium a, "bulk modulus" B, and its pressure derivative $B' = dB/dp$. It was found that u and η are rather insensitive to changes in a around the minimum. To the precision of our calculation, the total energy at each a thus corresponds to the minimum with respect to u and η and provides the correct bulk modulus corresponding to hydrostatic deformation.

IV. RESULTS

A. Total energy

In Tables I and II, we present the results of our structural relaxation calculations: the a, η, and u. In addition, the two bond lengths, the corresponding sums of Pauling radii, and the "ideal" bond lengths are listed. We notice that the equilibrium u values, which have an estimated uncertainty of ± 0.01, are close to 0.3 in all cases (in agreement with the experimental data for $MgSiP_2$). They thus differ significantly from the ideal value of 0.25. The tendency towards shorter C-V, Si-V than Be-V, Mg-V bond lengths is in agreement with what is expected from Pauling's ionic radii. The only exception $d_{\text{Be-N}} > d_{\text{Si-N}}$ can be understood from the fact that Be is less ionic (and hence has a larger radius) here than in the Be-VI compounds (used in Pauling's determination of the ionic radii) and that Si is partially ionic (and hence has a smaller radius than neutral Si).

Quantitatively, we see that neither the sum of atomic (i.e., Pauling) radii nor the bonds lengths for the ideal structure accurately matches the calculated first principles values for the case of the ternary nitrides. Only for $MgSiP_2$ do the sums of Pauling radii yield satisfactory agreement. The above conclusion for the nitrides differs from that for the other pnictides (P, As, and Sb) found in previous studies of the II-IV-V_2 semiconductors.[10,9] The calculated c/a values are on the other hand close to the ideal value of 2. For $MgSiP_2$, the reported experimental value is significantly smaller. Further theoretical work (with a full potential approach) and also additional measurements would be desirable. We note that the energies as functions of η for the various compounds have very shallow minima. This makes a precise determination of this parameter rather difficult. On the other hand, we obtained an excellent agreement with the experimental bond lengths for $BeSiN_2$ (Ref. 5) and $MgSiN_2$ (Ref. 6), which as we noted above have the wurtzitelike structure. This can be understood from the fact that the short-range atomic surroundings in the wurtzitelike crystal structure of these compounds, which were observed experimentally, are essentially the same as in the chalcopyrite structure. That is, in both these structures we

TABLE I. Structural properties. $d^p_{\text{IV-V}}$ and $d^p_{\text{II-V}}$ are the sums of Pauling radii of the corresponding elements; d_i is the calculated bond length for the ideal chalcopyrite structure.

II-IV-V_2	a (Å)	u	η	$d_{\text{IV-V}}$ (Å)	$d_{\text{II-V}}$ (Å)	$d^p_{\text{IV-V}}$ (Å)	$d^p_{\text{II-V}}$ (Å)	d_i (Å)
$BeCN_2$	3.71	0.30	1.96	1.50	1.71	1.47	1.76	1.61
$MgCN_2$	4.11	0.32	1.84	1.58	1.92	1.47	2.10	1.78
$BeSiN_2$	4.10	0.29	2.04	1.70	1.88	1.87	1.76	1.78
Expt.[a]				1.76	1.76			
$MgSiN_2$	4.44	0.31	1.96	1.77	2.08	1.76	2.10	1.92
Expt.[b]				1.76	2.08			
$MgSiP_2$	5.64	0.30	1.94	2.26	2.59	2.27	2.50	2.44
Expt.[c]	5.72	0.29	1.77	2.25	2.53			

[a] Experimental values for $BeSiN_2$ (Ref. 5).
[b] Experimental values for $MgSiN_2$ (Ref. 6).
[c] Experimental values for $MgSiP_2$ (Ref. 21).

have similar AN_4, SiN_4, and NSi_2A_2 atomic tetrahedra where A=Be,Mg. We believe that this local structure is the most important factor in determining the structure and electronic properties of the $BeSiN_2$ and $MgSiN_2$ compounds.

The cohesive and elastic properties of the ternary compounds and of the "parent" zinc-blende compounds along with the energies of relaxation from the ideal structure are listed in Table II. We note that the relaxation energies associated with the deviation from the ideal structure are significant, particularly for the compounds containing C. The cohesive energies per atom and bulk moduli of the ternaries are close to those for their "parents" while those for $MgCN_2$, $BeSiN_2$, and $MgSiN_2$ are closer to those for AlN than those for c-BN. We note that in general $MgCN_2$ and $BeSiN_2$ have properties closer to those of AlN than those of c-BN. $MgSiN_2$ is best lattice matched to AlN and has a lattice constant in between AlN (4.37 Å) and GaN (4.49 Å).

B. Electronic band structures

The band structures are shown in Figs. 1–4. It is useful to compare the band structures of $BeCN_2$ and $MgSiN_2$ with those of their "parents" c-BN and ZB-AlN displayed in the same bct Brillouin zone. The band structures for $BeSiN_2$ and $MgCN_2$ are compared with that for $AlBN_2$ with the ideal chalcopyrite structure and a lattice constant $a = 4.07$ Å, the average of lattice constants for BN and AlN. The band structures of III-V compounds are labeled using the notations for the zinc-blende Brillouin zone (BZ) and symmetry. The folding effects and relations between symmetry points of the BZ are illustrated in Fig. 5 (the notation follows Ref. 7). The point Z_{bct} $(0, 0, \pi/a)$ is equivalent to the point $(2\pi/a, 0, 0)$ labeled D in the adjoining BZ since they are related by a reciprocal lattice vector. A reflection of this is the symmetry of the bands of the line ZD about its midpoint N which is on the zone boundary. The Γ-X_{fcc} bands are folded on Γ-Z_{bct}. Thus, at Z_{bct} one finds both the eigenvalues which occur at the center of the Δ_{fcc} line and at the X_{fcc} point. At the Γ point, one finds Γ, X_{fcc}, and W_{fcc} eigenvalues. The folding of W_{fcc} onto Γ is a consequence of the superlattice ordering along {201}. At X_{bct}, one finds the L_{fcc} point and the point along Σ_{fcc}, $2\pi/a(\kappa, \kappa, 0)$ with $\kappa = 1/2$.

A rather unusual feature of all these band structures except the one for $BeCN_2$ is that the valence-band maximum does not occur at the Γ point for the relaxed configurations and even for the ideal $MgSiN_2$. This is also

TABLE II. Cohesive and elastic properties.

II-IV-V_2	E_{coh}[a] (eV/atom)	E_{rel}[b] (eV/atom)	B (GPa)	B'
c-BN	7.9		412	3.6
$BeCN_2$	7.7	1.2	333	3.8
ZB-AlN	6.3		220	3.9
$MgSiN_2$	5.7	0.6	195	4.0
$AlBN_2$	6.1		247	3.9
$MgCN_2$	5.1	0.8	210	2.9
$BeSiN_2$	6.1	0.2	240	3.9
ZB-AlP	4.3		83	4.1
$MgSiP_2$	3.8	0.3	75	4.3

[a]Cohesive energy (eV/atom) with respect to neutral atoms in their spin polarized LDA ground state. Zero point motion is not included.
[b]Relaxation energy (eV/atom): E_{coh} for the relaxed structure minus E_{coh} for the ideal chalcopyrite structure.

found to be the case for ZB-AlN. The positions of the maxima (k_{max}) and their difference $\delta E = E^v_{max}(k_{max}) - E^v_{max}(\Gamma)$ from the maximum at Γ are summarized in Table III. In view of the uncertain precision of the ASA for distorted structures, we consider only the differences for $MgCN_2$ and $MgSiN_2$ to be significantly above the error bar. The origin of the shift from Γ can be traced back to the very flat heavy hole band along the Σ_{fcc} direction for the III-V compounds. The maxima along the Γ-D axis occur close to the intersection (at A) of the Σ_{fcc} line with the line $(k_x, 0, \pi/a)$, which is folded onto the bct Γ-D line (see Fig. 5). For ZB-AlN, one sees a local maximum in the bands near this point. An additional local maximum in the valence bands occurs near the point B in Fig. 5. The exact k-space location of the valence-band maximum is sensitive to the relaxations: For $MgCN_2$, $BeSiN_2$, and $MgSiP_2$ the maxima for the ideal structure occur at the Γ point, while for the ideal $MgSiN_2$ it occurs at $(0.25, 0.25, 0)2\pi/a$.

Table III also summarizes the locations of conduction-band minima. The situation is similar for all compounds considered except $MgSiP_2$. One can see that for c-BN and ZB-AlN the conduction-band minima at the Γ and D points are degenerate, because they both correspond to the folded X^{ZB}_{1c} state. This degeneracy is almost fulfilled also for the "ideal" ternary nitrides. In the case of $MgSiP_2$ we have three almost degenerate conduction band minima at the Γ, X, and D points. But as is evident in the figures, this near degeneracy disappears in the relaxed structures. As a result, the conduction-band

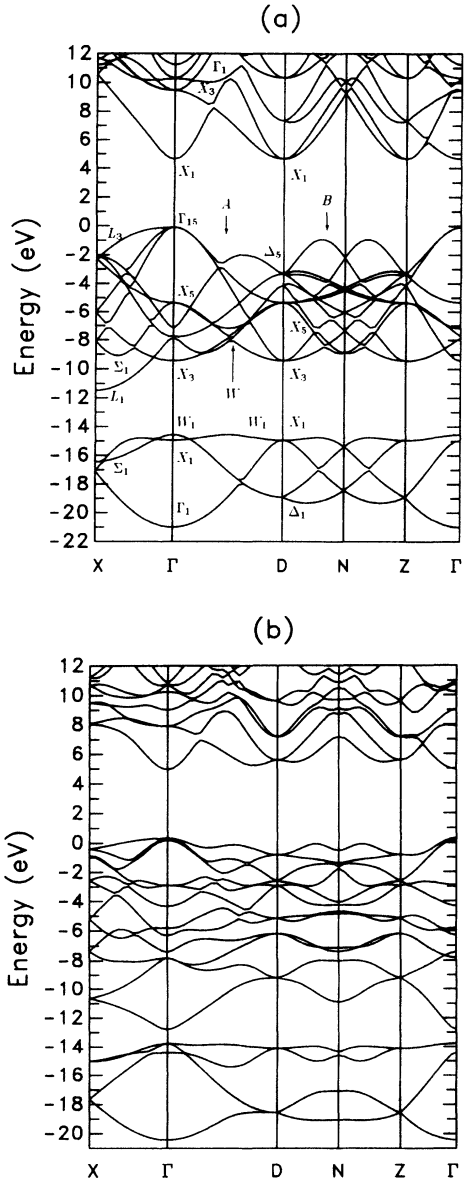

FIG. 1. Electronic band structure of the "parent" zinc-blende compound c-BN plotted in the Brillouin zone for the bct structure (a) and the "derived" ternary compound $BeCN_2$ (b). See Fig. 5 for labeling.

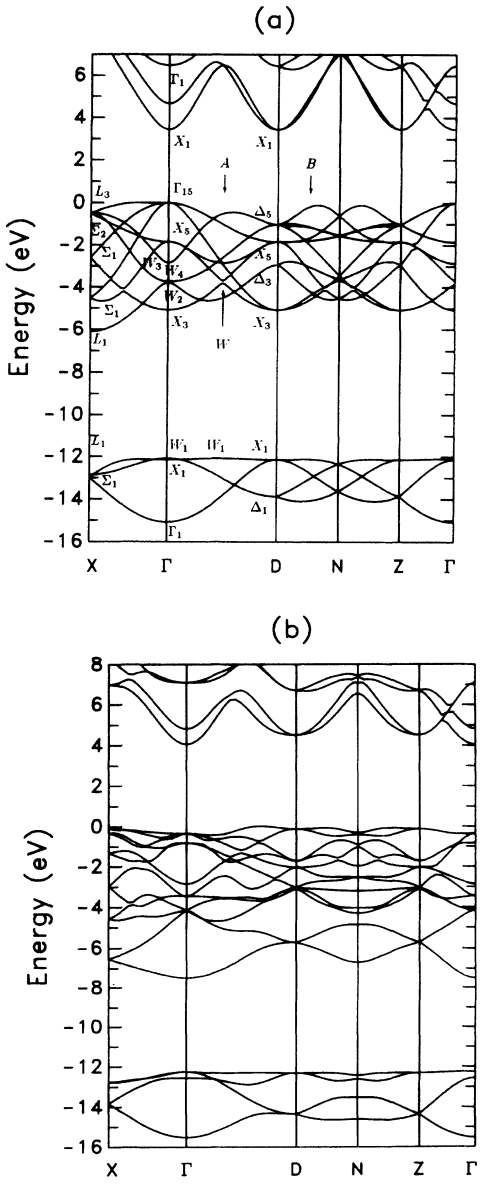

FIG. 2. Electronic band structure of the "parent" zinc-blende compound AlN plotted in the Brillouin zone for the bct structure (a) and "derived" ternary compound $MgSiN_2$ (b). See Fig. 5 for labeling.

TABLE III. Location in k space of the valence-band maxima and conduction-band minima and the energy difference in the upper valence band at the maximum and at the Γ point.

Compound	k_{max} $(2\pi/a)$	δE above Γ (meV)	k_{min} $(2\pi/a)$
c-BN	(0,0,0)		(0,0,0),(1,0,0)
$BeCN_2$(ideal)	(0,0,0)		(0,0,0),(1,0,0)
$BeCN_2$(relaxed)	(0,0,0)		(0,0,0)
ZB-AlN	(0.12,0.12,0)	4	(0,0,0),(1,0,0)
$MgSiN_2$(ideal)	(0.25,0.25,0)		(0,0,0),(1,0,0)
$MgSiN_2$(relaxed)	(0.7,0,0)	360	(0,0,0)
$AlBN_2$	(0,0,0)		(0,0,0),(1,0,0)
$MgCN_2$(ideal)	(0,0,0)		(0.9,0,0)
$MgCN_2$(relaxed)	(0.7,0,0)	242	(0,0,0)
$BeSiN_2$(ideal)	(0,0,0)		(0,0,0),(1,0,0)
$BeSiN_2$(relaxed)	(0.22,0.22,0)	33	(0,0,0)
AlP	(0,0,0)		(0,0,0),(1,0,0)
$MgSiP_2$(ideal)	(0,0,0)		(0.9,0,0)
$MgSiP_2$(relaxed)	(0.6,0,0)	77	(0.8,0,0)

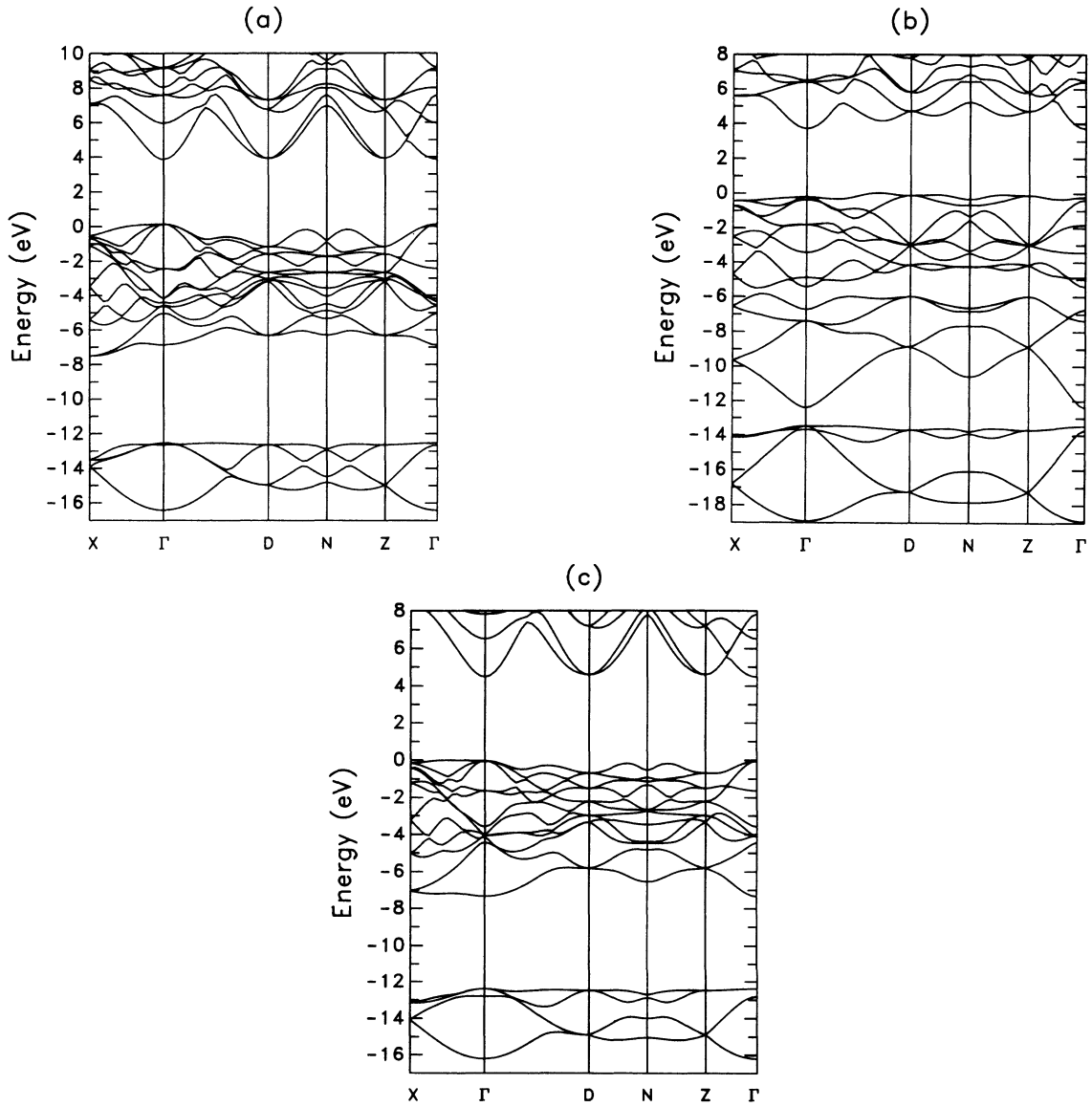

FIG. 3. Electronic band structure of the "parent" compound $AlBN_2$ (a) and "derived" ternary compounds $MgCN_2$ (b) and $BeSiN_2$ (c).

minimum is found at Γ_{bct} for all ternary compounds considered except $MgSiP_2$. For the "parent" materials c-BN, ZB-AlN, and AlP, however, the conduction-band minima occur at the X_{fcc} point.

It is clear that the strength of the "pseudodirect" ($\Gamma^v_{max} \rightarrow \Gamma^c_{min}$) optical transition depends on the amount by which Be(Mg)-C(Si) substitution for B or Al leads to a significant breaking of the zinc-blende symmetry and, as a result, the lifting of the forbiddeness associated with the indirect transition. The perturbation reflects both the nonvanishing difference between the potentials of the group-II and group-IV elements and the structural deviation from the "ideal," or zinc-blende, structure. The significant changes in the band structure between c-BN, ZB-AlN, and ZB-AlP and their "derived" ternaries indicates that the perturbation must be reasonably strong. One can see these from Table IV which summarizes the influence of the lattice relaxation on the energies of different conduction-band minima relative to the valence-band maximum in each of the ternary compounds. The perturbation is thus also expected to lead to reasonably strong optical transitions at the direct band gap. Indeed, the perturbation potential due to Be(Mg)-C(Si) substitution for B or Al possesses the tetragonal symmetry of the group of X_{fcc}. This perturbation alone seems to be sufficiently strong to provide significant mixing of the Γ^c_1 and X^c_1 conduction-band states of the corresponding "parent" compound even in the absence of the lattice relaxation. Moreover, the same potential induces large anion displacements toward the group-IV elements. One can represent these displacements as a superposition of frozen phonons of different equivalent W points

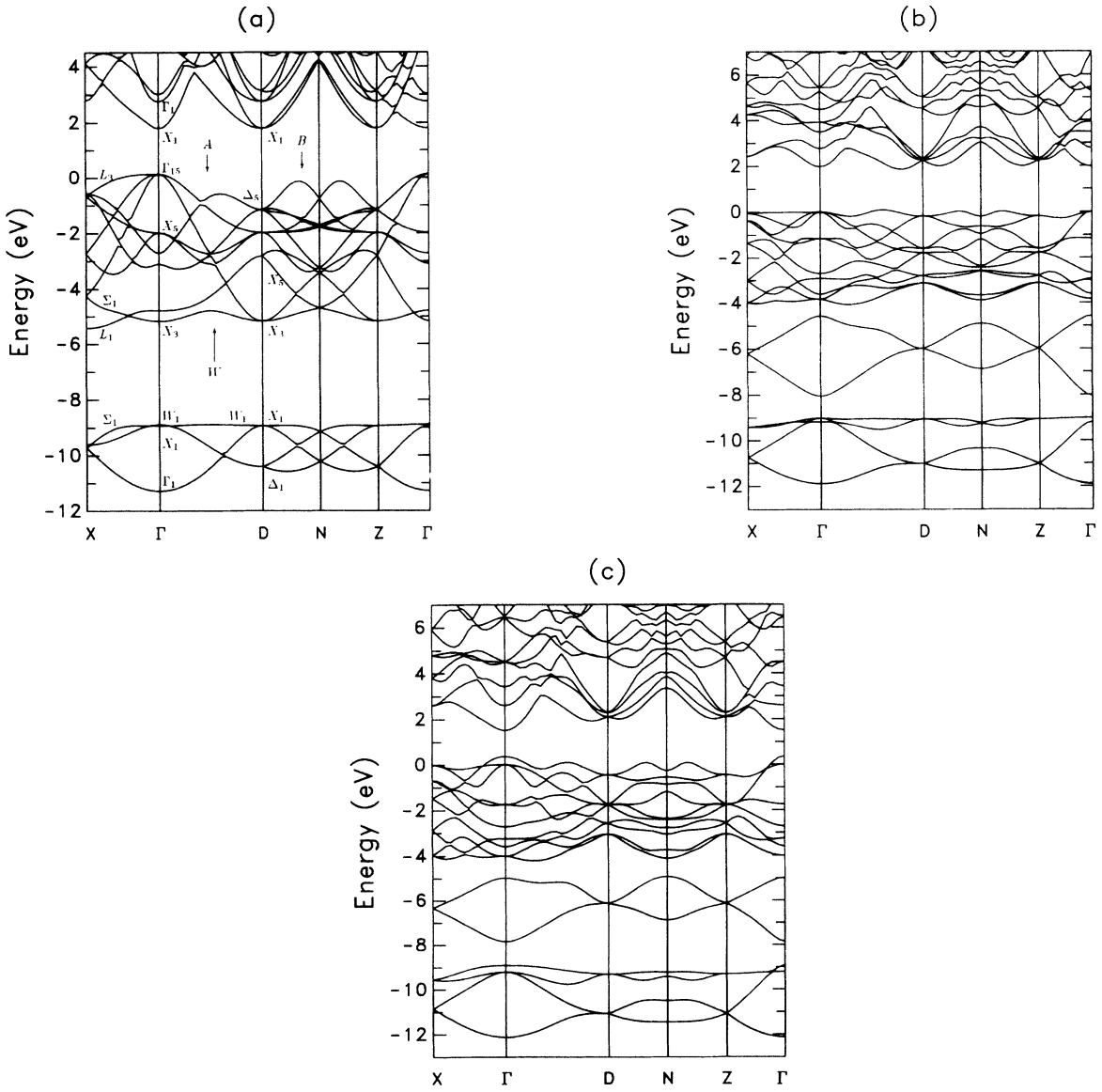

FIG. 4. Electronic band structure of the "parent" zinc-blende compound AlP plotted in the Brillouin zone for the bct structure (a) and "derived" ternary compound $MgSiP_2$ for calculated (b) and experimental (c) structure parameters. See Fig. 5 for labeling.

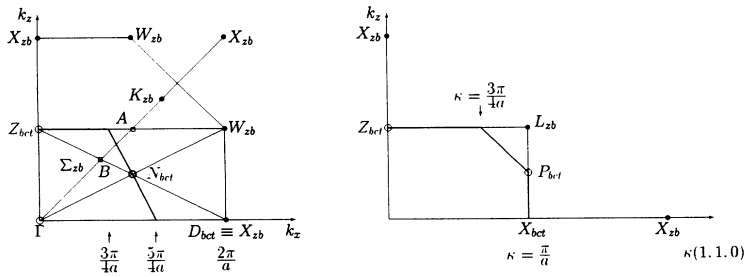

FIG. 5. Relation between the zinc-blende (fcc) and chalcopyrite (bct) Brillouin zone symmetry k points. The notation follows Ref. 7.

of the fcc Brillouin zone. The resulting frozen-phonon mode has the symmetry of the X_1^{zb} irreducible representation. An elementary group-theoretical analysis shows that this frozen-phonon perturbation leads to the further mixing of Γ_1^c and X_1^c states. Thus we can expect reasonably strong optical transition at the direct band gap in the ternary compounds due to the contribution from the Γ_{15}^v-Γ_1^c dipole transition of the corresponding "parent" compound. We note, however, that while the $\Gamma_1^c - X_1^c$ splitting in ZB-AlN is only 1.1 eV it is 6.0 eV in c-BN. Thus, we can expect a larger mixing and hence larger dipole matrix element for the direct optical transition in the AlN-derived compounds than in $BeCN_2$. The lowest conduction state at Γ is actually Γ_{15}^c, which does not mix with X_1^c in first-order perturbation theory.

This fact may have special interest for $BeCN_2$ which has lattice parameters, elastic constants, and electronic structure that are rather close to those of c-BN. On the other hand, this direct-band-gap semiconductor evidently has superior optical properties compared to those of c-BN. In fact, all carbo- and siliconitrides have their absolute conduction band minima at the Γ point due to strong lattice distortions (see Table IV). We note that only in $BeSiN_2$ are the energies of the minima at Γ and Z_{bct} nearly equal (as they are exactly in AlN). In other materials, however, the minima at Γ are $\sim$0.5–1 eV lower than those at Z_{bct}, thus indicating a stronger perturbation of this state.

For $MgSiP_2$, the conduction-band minimum is found at $(0.8, 0, 0)2\pi/a$ for the relaxed structure and near the X_{bct} point for the ideal structure. The conduction-band minimum of the relaxed structure bears a resemblance to the second lowest minimum in $BeCN_2$, which lies a bit closer to the $D \equiv Z$ point. At that point, all the bands are doubly degenerate because of the presence of a nonsymmorphic space-group symmetry element in the group of the k point. This is the origin of the shift of the minimum away from D. This situation is reminiscent of the Δ minima of the Si and diamond-C band structures. The valence-band maxima along the line Γ-D may have a similar correlation to the nonsymmorphic nature of the space group.

Because the majority of valence-band maxima (and for $MgSiP_2$ also the conduction-band minimum) do not occur at Γ, the materials of concern here (except for $BeCN_2$) are predicted to have slightly smaller *indirect* gaps than the direct, or "pseudodirect," gaps discussed above. The fact that there are several valence-band maxima and conduction-band minima closely spaced in energy but at different k points may have significant effects on the p- and n-type transport, the optical emission and absorption properties, and the nature of shallow defect states.

We note that for the relaxed $MgSiP_2$ band structure, the lowest band gap, although not at Γ, is close to direct since the valence-band maxima and conduction-band minima occur at close-lying k points. This means that small q, low-energy phonons would be involved in the band-edge optical transitions. In contrast, we note that the band gap for the experimental structure parameters

TABLE IV. Calculated conduction-band minima (eV) with respect to the valence-band maxima at different symmetrical points.

Compound	Γ	D	X
c-BN	4.73	4.73	10.66
$BeCN_2$(ideal)	4.21	4.24	5.96
$BeCN_2$(relaxed)	4.63	5.24	7.76
ZB-AlN	3.44	3.44	7.86
$MgSiN_2$(ideal)	3.44	3.36	5.40
$MgSiN_2$(relaxed)	4.03	4.50	6.96
$AlBN_2$	3.71	3.77	6.96
$MgCN_2$(ideal)	3.04	2.85	2.97
$MgCN_2$(relaxed)	3.69	4.68	5.57
$BeSiN_2$(ideal)	3.60	3.60	7.55
$BeSiN_2$(relaxed)	4.47	4.60	8.23
ZB-AlP	1.65	1.65	2.65
$MgSiP_2$(ideal)	1.73	1.47	1.63
$MgSiP_2$(relaxed)	1.88	2.16	2.34

[Fig. 4(c)] is, in fact, direct at Γ. This illustrates the significant effects that relaxation produces in the band structure of these materials. The minimum band gaps are summarized in Table V.

It is of interest to consider the magnitude and the origin of the difference between the band gaps for the ternary compounds and their "parents." The change in the gap ΔE_g can be divided into two terms: one $\Delta E_g^{\rm chem} = E_g(\text{ideal}) - E_g(\text{parent})$ is due to the replacement of the two group-III atoms in the enlarged cell by a group-II atom and a group-IV atom in the ideal structure, and the second $\Delta E_g^{\rm rel} = E_g(\text{relaxed}) - E_g(\text{ideal})$ is due to the relaxation. As can be seen from the Table V, where these quantities are listed, $\Delta E_g^{\rm chem}$ is negative and $\Delta E_g^{\rm rel}$ is positive in all cases. The total change is negative (i.e., the gap is reduced) in the two compounds containing carbon and positive in the remaining three. A part of $\Delta E^{\rm chem}$—generally small—arises from the splitting of the threefold-degenerated valence-band maximum at Γ in the zinc-blende compounds. The fact that the relaxation tends to widen the gap is due to the increased bonding-antibonding splitting associated with the enhanced interaction due to the displacement of the anion towards the group-IV atom. In addition, the shifts in the locations of the extrema also have an effect on $\Delta E_g^{\rm rel}$.

As an example of the local density of states (DOS) for the compounds investigated, Fig. 6 shows those for $MgSiN_2$ both for the ideal (dashed curves) and for the relaxed (solid curves) configurations. To be noted are the significantly different ordinate scales used for the N, Si, and Mg panels. The lower valence bands, which lie between −12.5 eV and −15.5 eV and are largely N 1*s*-like, are omitted. Clearly, the N orbitals are dominant in the valence bands while the Si DOS are larger than those for Mg in the valence and lower conduction bands. The increase in band gap due to the relaxation is evident. The latter consists mainly of a displacement of the N towards the Si and away from the Mg ($u > 0.25$). Associated with this is the expected increase (decrease) in the Si(Mg) DOS in the valence bands and the reverse occurring in the lower conduction bands.

The LDA is well known to underestimate the band gaps. For wurtzite AlN, for example, our calculated LDA

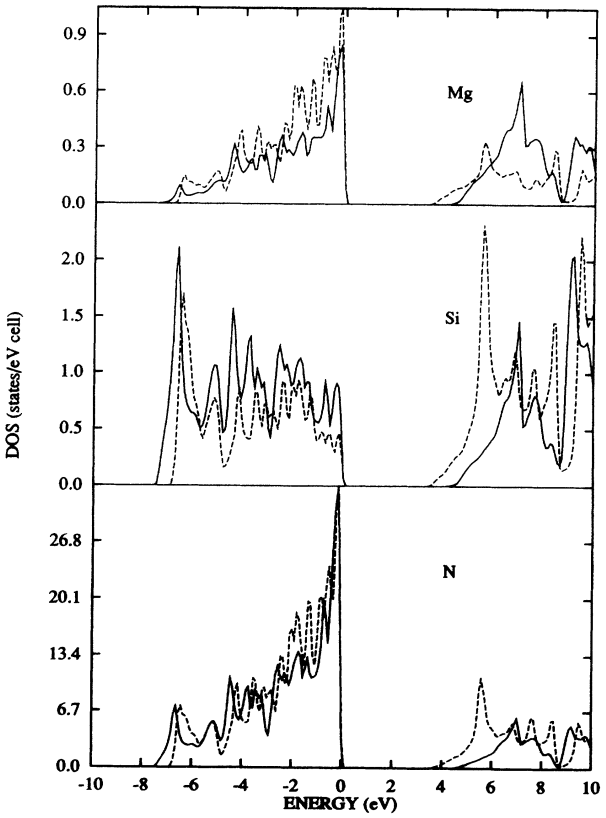

FIG. 6. Calculated local densities of states of $MgSiN_2$ in the ideal (a) and relaxed (b) chalcopyrite structures.

gap[23] is 4.9 eV while the experimental gap is 6.2 eV. Thus, we can expect a 1.3±0.5 eV correction for $MgCN_2$, $BeSiN_2$, and $MgSiN_2$. For ZB-AlN, the LDA gap was found to be 3.4 eV.[23] A simple scheme suggested by Bechstedt and del Sole[24] for estimating GW corrections to the LDA band gaps provides a reasonable agreement with experimental band gaps for most of the $A_N B_{8-N}$ compounds. The corrected band gaps are summarized in Table V. The experimental value of 4.8 eV for the $MgSiN_2$ band gap reported in the literature[25] is not too far below our estimated value of 5.3 eV. The reported value,[25] be-

TABLE V. Calculated (LDA) band gaps (in eV), estimated band gaps with "*GW*" corrections included, and band gap shifts due to atomic substitution and lattice relaxation.

Compound	LDA (ideal)	LDA (relaxed)	"*GW*" (relaxed)[a]	$\Delta E_g^{\rm chem}$ [b]	$\Delta E_g^{\rm rel}$ [b]	$\Delta E_g^{\rm tot}$
c-BN	4.73		6.4			
$BeCN_2$	4.22	4.62	6.3	-0.51	0.40	-0.11
ZB-AlN	3.44		4.7			
$MgSiN_2$	3.36	4.03	5.3	-0.08	0.67	0.59
$AlBN_2$	3.71		5.0			
$MgCN_2$	2.83	3.69	5.0	-0.88	0.86	-0.02
$BeSiN_2$	3.60	4.47	5.7	-0.11	0.87	0.76
ZB-AlP	1.65		2.3			
$MgSiP_2$	1.47	1.77	2.5	-0.18	0.30	0.12
$MgSiP_2$ (expt.)		1.20				

[a]Calculated according to Ref. 24.

[b]Defined in text.

ing based on photoluminescence measurements, may well be an underestimate and needs further verification. We note that $BeCN_2$ and c-BN and $MgCN_2$ and ideal $AlBN_2$ have almost equal band gaps. The two other ternary nitrides, however, have larger band gaps than the corresponding group-III nitride. Superlattice structures based on the hexagonal wurtzite structure instead of the cubic ZB structure conceivably might have lower total energies for these rather ionic compounds. Since wurtzite AlN has a direct band gap, the compounds with these structures might also have larger and conceivably strongly direct gaps in contrast to the "pseudodirect" band gaps considered here. (Recall, however, that the argument given above indicates that the optical matrix element is not expected to be very weak for the zinc-blende-based structures.) Further work will be necessary to study this possibility.

For $MgSiP_2$, Continenza *et al.*[9] obtained a smaller minimum band gap (1.16 eV) which is direct at Γ. This discrepancy results from the difference in structure used. They used the experimental c/a value and only minimized the total energy with respect to u. At the experimental lattice parameters, we obtained a direct gap at Γ of 1.13 eV, in agreement with their result. However, it should be noted that our calculated total energy is of the order of 0.2 eV/atom higher at the experimental lattice parameters than at the theoretical equilibrium. As noted in Sec. IV A, full-potential calculations will be required to determine the structural parameters with high confidence. It is interesting to note that the band structures are sensitive to these structural changes. Similar uncertainties probably also exist for the other ternary compounds investigated here.

V. CONCLUSIONS

The main general conclusions of this work are the following: (1) The properties of $BeCN_2$, $MgSiN_2$, $MgSiP_2$, and $MgCN_2$ and $BeSiN_2$ in the chalcopyrite structure are similar to those of their respective "parents" BN, AlN, AlP (in the zinc blende structure), and $AlBN_2$ (in the ideal chalcopyrite structure); (2) the properties of $MgCN_2$ and $BeSiN_2$ are more similar to those of AlN than BN; and (3) $BeCN_2$ is a direct-band-gap semiconductor in contrast to BN. The fully relaxed structures found by the first principles calculations exhibit significant distortions from the ideal chalcopyrite structure leading to shorter Si-anion and C-anion bond lengths and longer Be-anion and Mg-anion bonds. The result for $MgSiP_2$ is in fair agreement with experiment. However, we obtained an excellent agreement with experimental data for the bond lengths in $BeSiN_2$ and $MgSiN_2$ which were synthesized in a wurtzitelike structure having the same short-range order as the chalcopyrite form. We found in general that the calculated bond lengths are not accurately given by the sum of atomic (e.g., Pauling) radii nor by the values for the ideal structures.

We found that all compounds studied have conduction-band minima at the center of the Brillouin zone for the body centered tetragonal lattice. These minima correspond to the $X_{\rm fcc}$ folded states in the fcc Brillouin zone of the "parent" compounds. Except for $BeCN_2$, all the ternary compounds studied are found to have the maximum of the valence band away from Γ, and as a result are indirect. This unusual behavior was found to be related to the very flat upper valence band for the "parents" along the $\Sigma^{\rm ZB}$ direction. The minimum direct transition at Γ is "pseudodirect" since in all zinc-blende "parents" it is an indirect transition from Γ to a zone boundary $X_{\rm fcc}$ folded state. Nevertheless, this transition is expected to be reasonably strong because of the significant difference in potentials between the group-II and group-IV elements, which breaks the zinc-blende symmetry, and because of the additional mixing of $\Gamma_1^{\rm ZB}$ and $X_1^{\rm ZB}$ states due to the lattice distortion.

ACKNOWLEDGMENTS

This work was supported by ONR-Grant No. N-00014-89-J-1631 and NSF Grant No. DMR-92-22387.

[1] *Wide Band Gap Semiconductors*, edited by T. D. Moustakas, J. I. Pankove, and Y. Hamakawa, MRS Symposia Proceedings No. 242 (Materials Research Soceity, Pittsburgh, 1992).

[2] G. C. Xing, K. J. Bachmann, J. B. Posthill, and M. L. Timmons, in *Diamond, Silicon Nitride, and Related Wide Bandgap Semiconductors*, edited by J. T. Glass, R. Messier, and N. Fujimori, MRS. Symposia Proceedings No. 162 (Materials Research Society, Pittsburgh, 1989), p. 615, and references therein.

[3] B. F. Levine, Phys. Rev. B **7**, 2600 (1973).

[4] O. Alerhand, R. D. Meade, T. Arias, and J. D. Joannopoulos, Bull. Am. Phys. Soc. **37**, 665, abstract O25.2 (1992).

[5] P. Eckerlin, Z. Anorg. Allgem. Chem. **353**, 225 (1967).

[6] M. Winterberger, F. Tcheou, J. David, and J. Lang, Z. Naturforsch. B **35**, 604 (1980).

[7] C. J. Bradley and A. P. Cracknell, *The Mathematical Theory of Symmetry in Solids: Representation Theory For Point Groups and Space Groups* (Clarendon Press, Oxford, 1972).

[8] W. R. L. Lambrecht and B. Segall, Phys. Rev. B **45**, 1485 (1992).

[9] A. Continenza, S. Massida, A. J. Freeman, T. M. de Pascale, F. Meloni, and M. Serra, Phys. Rev. B **46**, 10 070 (1992).

[10] J. E. Jaffe and A. Zunger, Phys. Rev. B **29**, 1882 (1984).

[11] A. Zunger and J. E. Jaffe, Phys. Rev. Lett. **51**, 662 (1983).

[12] P. Hohenberg and W. Kohn, Phys. Rev. **136**, B864 (1964); W. Kohn and L. J. Sham, *ibid.* **140**, A1133 (1965).

[13] L. Hedin and B. I. Lundqvist, J. Phys. C **4**, 2064 (1971).

[14] For a recent account, see O. K. Andersen, O. Jepsen, and M. Šob, in *Electronic Band Structure and its Applications*, edited by M. Yussouff (Springer, Heidelberg, 1987).

[15] Originally introduced by D. Glötzel and O. K. Andersen

(unpublished); see Ref. 14 for a discussion.
[16]D. Glötzel, B. Segall, and O. K. Andersen, Solid State Commun. **36**, 403 (1980).
[17]H. J. Monkhorst and J. D. Pack, Phys. Rev. B **13**, 5188 (1976).
[18]N. E. Christensen and S. Satpathy, Phys. Rev. Lett. **55**, 600 (1985); N. E. Christensen, Phys. Rev. B **32**, 207 (1985).
[19]H. L. Skriver, Phys. Rev. B **31**, 1909 (1985); A. K. McMahan, H. L. Skriver, and B. Johansson, *ibid.* **23**, 5016 (1981).
[20]P. Blöchl, Ph.D. thesis, Stuttgart University, Stuttgart 1989.
[21]A. A. Vaipolin, Fiz. Tverd. Tela (Leningrad); **15**, 1430 (1973) [Sov. Phys. Solid State **15**, 965 (1973)].
[22]J. H. Rose, J. R. Smith, F. Guinea, and J. Ferrante, Phys. Rev. B **29**, 2963 (1984).
[23]W. R. L. Lambrecht and B. Segall, in *Wide Band-Gap Semiconductors* (Ref. 1), p. 367; Phys. Rev. B **43**, 7070 (1991).
[24]F. Bechstedt and R. del Sole, Phys. Rev. B **38**, 7710 (1988).
[25]G. K. Gaido, G. P. Dubrovskii, and A. M. Zykov, Izv. Akad. Nauk. SSSR, Neorg. Mater. **10**, 564 (1974).